Supplementary Information

Ligand exchange triggered controlled-release targeted drug delivery system based on core–shell superparamagnetic mesoporous microspheres capped with nanoparticles

Zhaogang Teng,[a] Xingang Zhu,[b] Gengfeng Zheng,[a] Fan Zhang,[a] Yonghui Deng,[a] Lichen Xiu,[a] Wei Li,[a] Qing Yang*[b] and Dongyuan Zhao*[a]

[a] Department of Chemistry, Shanghai Key Laboratory of Molecular Catalysis and Innovative Materials, Laboratory of Advanced Materials, Fudan University, Shanghai 200433, PR China.

[b] School of Life Sciences, Fudan University, 220 Handan Road, Shanghai 200433, PR China

Email: dyzhao@fudan.edu.cn; yangqing68@fudan.edu.cn, Tel: 86-21-5163-0205, Fax: 86-21-5163-0307

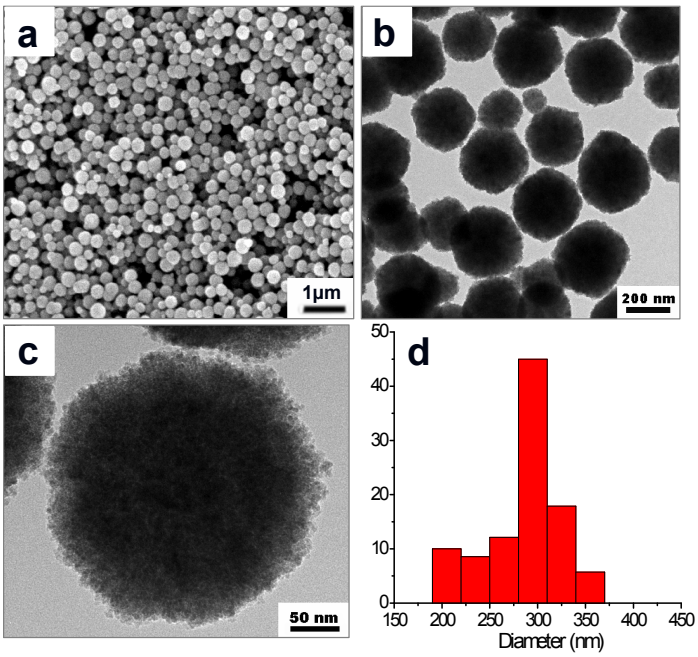

Figure S1. SEM (a) and TEM (b, c) images of magnetite spheres and the size distribution (d) of the spheres by measuring about 150 particles. The magnetite particles were synthesized by a solvothermal reaction. Briefly, 0.65 g of $FeCl_3$, 0.20 g of trisodium citrate dihydrate and 1.20 g of sodium acetate were dissolved in 20 ml of ethylene glycol under magnetic stirring. The obtained homogeneous yellow solution was transferred to a Teflon-lined stainless-steel autoclave with a capacity of ~ 30 ml. The autoclave was heated to 200 °C and maintained for 10 h, and then cooled down to room temperature. The obtained black magnetite particles were washed with water for 5 times, and then dried in vacuum at 60 °C for 12 h.

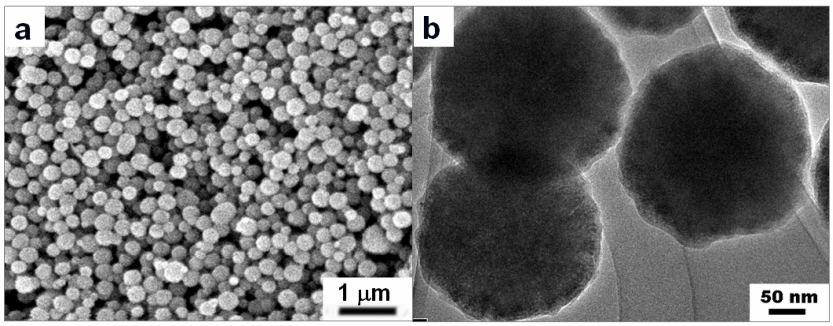

Figure S2. The SEM (a) and TEM (b) images of the core-shell Fe_3O_4@nSiO_2 spheres prepared using conventional Stöber method by dispersing the magnetite Fe_3O_4 spheres in 5.0 ml of concentrated ammonia aqueous solution (25 wt %), 160 μl of TEOS, 400 ml of ethanol, and 100 ml of deionized water.

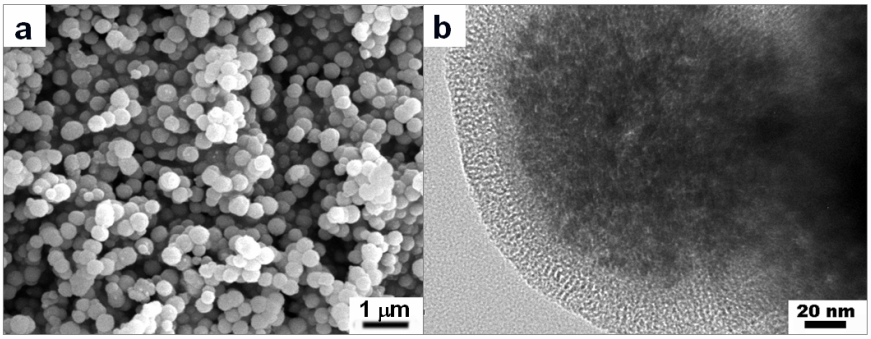

Figure S3. SEM (a) and TEM (b) images of the superparamagnetic mesoporous silica microspheres (SMMs) prepared by two-step coating procedures.

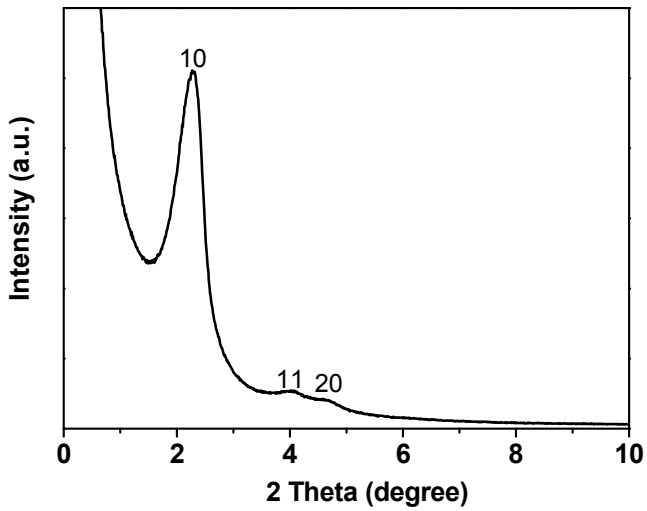

Figure S4. Low-angel XRD pattern of the superparamagnetic mesoporous microspheres.

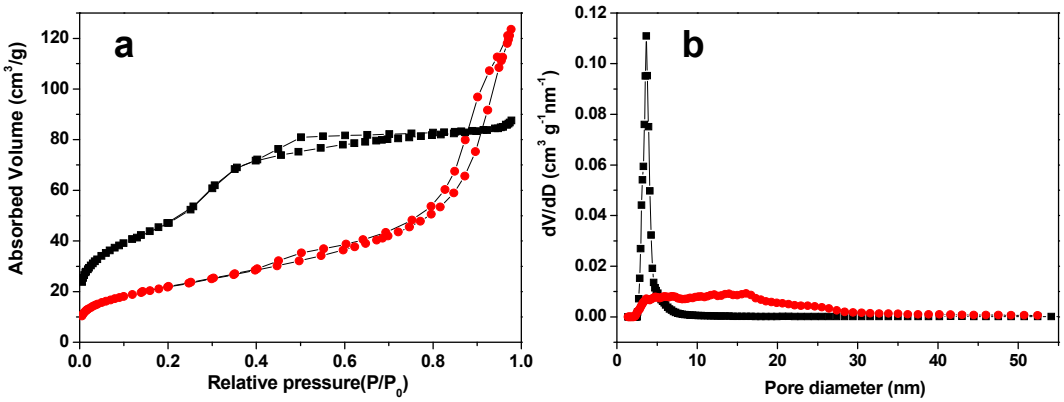

Figure S5. Nitrogen adsorption-desorption isotherms (a) and pore size distribution curves (b) of the superparamagnetic mesoporous silica microspheres (black) and SMM-IONP (red). The decrease of absorption volume at p/p_0 = 0.3 – 0.7 and the disappearing of the maximum peak in pore size distribution plot indicate that the mesopores of superparamagnetic mesoporous microspheres are capped by the iron oxide nanoparticles. The hysteresis loop of SMM-IONP at p/p_0 = 0.8 – 1 is attributed to the accumulation of iron oxide nanoparticles on the surfaces of microspheres.

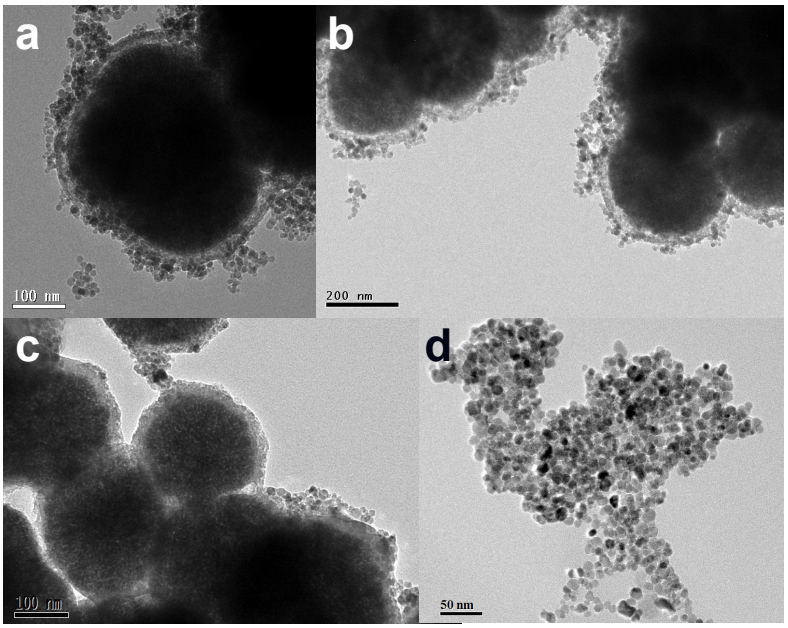

Figure S6. TEM images of the nanoparticles (Fe_3O_4) detached from the drug delivery system by addition of sodium citrate solution (20 mM) for 5 (a); 10 (b); and 15 min (c). The nanoparticles Fe_3O_4 detached from the drug delivery system surface after addition of sodium citrate for 15 min (d).

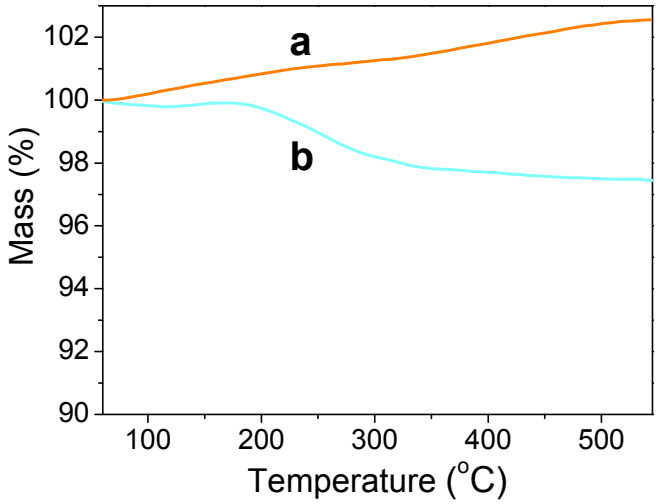

Figure S7. Thermogravimetric (TG) curves of the iron oxide nanoparticles before (a), and after (b) modified with iminodiacetic acid.

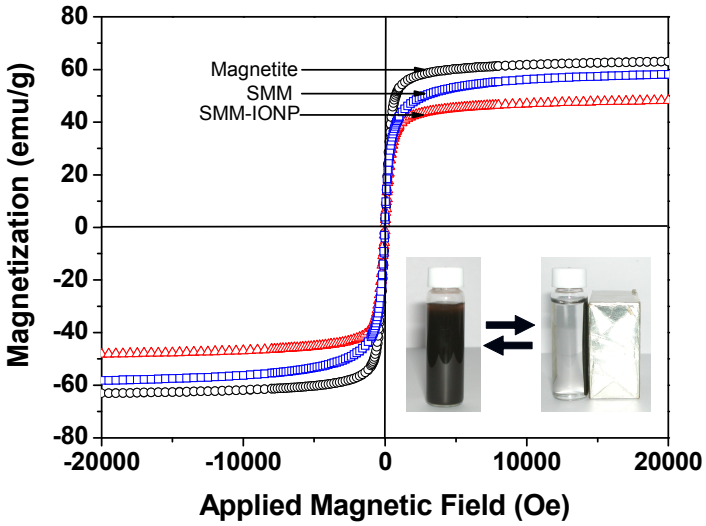

Figure S8. Room-temperature magnetization curves of the magnetite Fe_3O_4 spheres, superparamagnetic mesoporous silica microspheres (SMMs), and drug delivery system based on superparamagnetic mesoporous microspheres caped with iron oxide nanoparticles (SMM-IONP). Insert is the photographs of the captured drug delivery system by a 0.4 T magnet and the redispersed system by slight shaking after removal of the magnet.

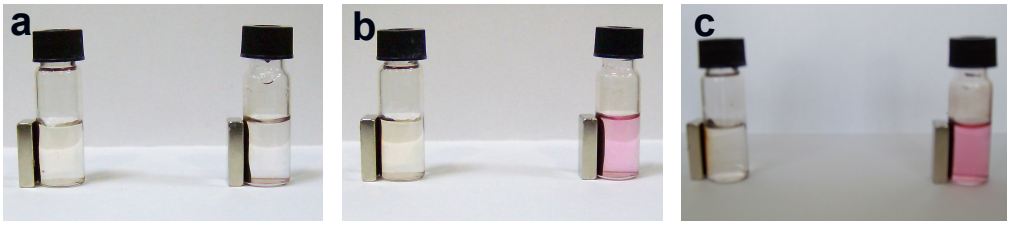

Figure S9. Photographs of two bottles charged with 15 mg of Rhodamine B-loaded drug delivery system dispersed in 2.0 ml of PBS solution. (a), The Rhodamine B-loaded drug delivery system collected by external magnets; (b) after the addition of (0.01 M) sodium citrate to the solution contained in the bottle on the right, pink fluorescence for 15 seconds. Showing a release of Rhodamine B from the encapsulated matrix; (c) after the addition of sodium citrate to the solution for 1.5 h.

Table S1. Means, standard deviations, and P-values of SGC-7901 cells incubated with the superparamagnetic mesoporous silica microspheres (SMMs) and drug delivery system (SMM-IONP) at different concentrations for 10 ~ 16 h.

		control	SMM 0.01 mg/ml	SMM 0.1 mg/ml	SMM-IONP 0.01 mg/ml	SMM-IONP 0.1 mg/ml
mean	10 h	1	0.965	0.864	0.985	0.842
standard deviation		0	0.106	0.111	0.079	0.050
P			0.610	0.083	0.765	0.007
mean	12 h	1	0.924	0.836	0.967	0.840
standard deviation		0	0.075	0.109	0.097	0.055
P			0.305	0.066	0.494	0.002
mean	16 h	1	0.973	0.847	0.974	0.845
standard deviation		0	0.103	0.108	0.042	0.064
P			0.658	0.037	0.399	0.003

Table S2. Means, standard deviations, and P-values of PC12 cell incubated with the superparamagnetic mesoporous silica microspheres (SMM) and drug delivery system (SMM-IONP) at different concentrations for 6 ~ 12 h.

		control	SMM 0.01 mg/ml	SMM 0.1 mg/ml	SMM-IONP 0.01 mg/ml	SMM-IONP 0.1 mg/ml
mean	6 h	1	0.923	0.730	0.890	0.712
Standard deviaton		0	0.118	0.110	0.050	0.078
P			0.253	0.003	0.019	0.000
mean	8 h	1	0.917	0.798	0.939	0.758
Standard deviaton		0	0.071	0.068	0.039	0.103
P			0.218	0.014	0.353	0.011
mean	12 h	1	0.937	0.750	0.899	0.772
Standard deviaton		0	0.084	0.084	0.099	0.061
P			0.259	0.001	0.171	0.007

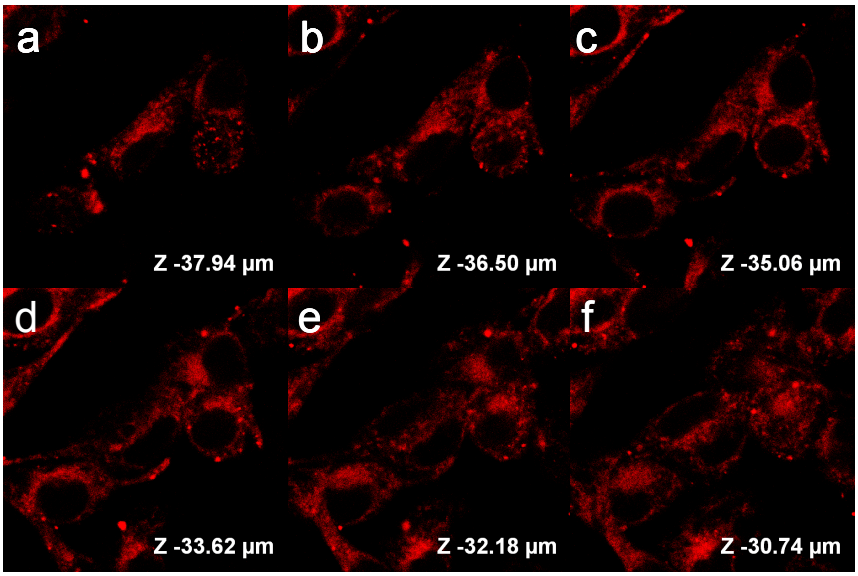

Figure S10. Fluorescence confocal micrographs of HeLa cells incubated with the rhodamine B-loaded drug delivery system. The focal plane was varied along the Z-axis from (a) the bottom to (f) the top of the cells. After incubated for 2 h, the micrographs of the live cells with different focal depth along Z-axis show that the rhodamine B-loaded drug delivery system is indeed internalized by HeLa cells.

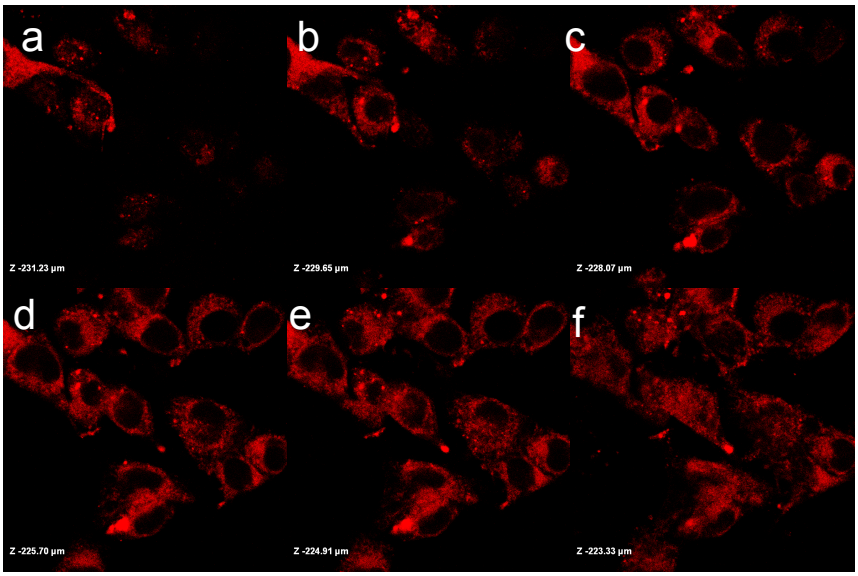

Figure S11. Fluorescence confocal micrographs of SGC-7901 cells incubated with the rhodamine B-loaded drug delivery system. The focal plane is varied along the Z-axis from (a) the bottom to (f) the top of the cells. After incubated for 2 h, the micrographs of the live cells with different focal depth along Z-axis show that the rhodamine B-loaded drug delivery system is indeed internalized by SGC-7901 cells.

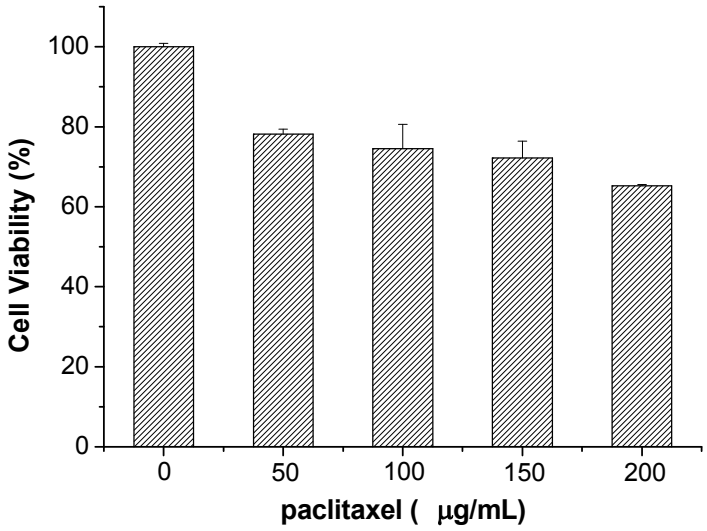

Figure S12. Viability of SGC-7901 cells incubated with free paclitaxel at different concentrations.